SSRG International Journal of Electronics and Communication Engineering
ISSN: 2348-8549/ https://doi.org/10.14445/23488549/IJECE-V13I1P116

Volume 13 Issue 1, 193-206, January 2026

Original Article

Autism Spectrum Disorder Detection using Enhanced 3D-ResNet50 Algorithm

P. Yugander[1], M. Jagannath[2]

[1,2] *School of Electronics Engineering, Vellore Institute of Technology, Chennai, Tamil Nadu, India.*

[2]*Corresponding Author : jagan.faith@gmail.com*

Received: 08 November 2025 Revised: 10 December 2025 Accepted: 09 January 2026 Published: 14 January 2026

Abstract - *Autism Spectrum Disorder (ASD) is a neuro-developmental disease that affects behavioural retardation in verbal communications and social interactions. Clinicians employ various ASD detection techniques to identify the condition. However, these traditional methods are time-consuming and suffer from a lack of accuracy. Over the last two decades, Machine Learning (ML) and Deep Learning (DL) algorithms have played a crucial role in the field of biomedical signal and image processing. In this paper, we propose a Machine Learning Framework. This contains two stages. In the first stage, an enhanced 3D-ResNet50 algorithm is proposed. The proposed algorithm is used to extract features from Magnetic Resonance (MR) Images. In the second stage, the extracted features are used to classify the ASD controls using Machine Learning Algorithms. To improve the accuracy of ASD classification, an enhanced 3D-ResNet50 algorithm is integrated with the ML algorithms. The proposed algorithm is used along with the machine learning algorithms like Support Vector Machine (SVM), K-Nearest Neighbours (KNN), Random Forest (RF), and Logistic Regression (LR). The proposed machine learning framework is tested on 1112 Functional Magnetic Resonance Images (fMRI). These images are collected from the Autism Brain Imaging Data Exchange (ABIDE-I) website. The ABIDE-I website provides a collection of 17 datasets from various international biomedical laboratories. The proposed algorithm is tested on the total ABIDE-I website and 17 individual datasets. Our proposed approach achieved 90% overall accuracy and 97% accuracy for the individual NYU dataset alone.*

Keywords - *Autism, 3D-ResNet50, Support Vector Machine, MR images, Random Forest.*

1. Introduction

Autism Spectrum Disorder (ASD) represents a challenging neurobiological disorder that affects how people connect socially, make relationships, and show behavioral adaptability. A correct diagnosis at an early stage is essential for successful treatments that yield positive developmental outcomes. Standard ASD diagnosis methods depend mainly on expert evaluations and behavioral monitoring, yet these methods require a lot of time and yield inconsistent results [1]. The new capabilities of neuroimaging combined with Artificial Intelligence (AI) technology now allow for an automated process in ASD diagnosis through objective and data-centric evaluation. The Magnetic Resonance Images (MRI), at their functional level, demonstrate exceptional power by examining connections in autistic brains to reveal more about ASD neurological origins [2]. Multiple challenges persist when using neuroimaging techniques for autism spectrum disorder diagnosis. The difficulty in developing machine learning applications stems from diverse imaging protocols and datasets between research facilities that reduce the extent to which machine learning models can be generalized. The high level of complexity, combined with multiple dimensions in Functional Magnetic Resonance Imaging (fMRI) data, prevents researchers from finding compelling discriminator features to separate ASD and control subjects [3]. Regular methods for extracting features from fMRI data by engineering handcrafted features with simple ML algorithms fail to detect the complex neuroimaging data patterns, leading to poor classification output. Better and more reliable approaches are essential to developing robust ASD classification systems that produce higher accuracy results [4]. Conventional approaches to ASD classification successfully use Convolutional Neural Networks (CNNs) and 3D CNNs to extract spatial and temporal features from fMRI data [5]. However, applying these models produces weak generalization results, particularly in multi-site datasets with different imaging standards. The diverse fMRI scan variations between institutions make it difficult to create models that apply consistently to various datasets. Experts must develop advanced approaches to process complex neuroimaging information while managing its built-in data variations. The proposed research presents a new hybrid framework that uses 3D-ResNet50 for deep feature extraction and ML algorithms like SVM, RF, KNN, and LR for classification operations [6]. The 3D-ResNet50 architecture extracts complex features

from fMRI data, enabling the ML classifier algorithms to achieve high-accuracy ASD classification through feature utilization. The proposed method uses 3DResNet-50 combined with traditional ML approaches because this framework overcomes traditional diagnosis methods while boosting ASD evaluation accuracy. The proposed framework achieves its evaluation through analysis of the publicly available ABIDE-I dataset that presents fusion data from 17 international sites for comprehensive model examination [7]. The experimental outcomes confirm that the proposed framework provides effective ASD classification by achieving superior performance [8].

The existing ASD identification methods are expertise-dependent and time-consuming. Over the past two decades, numerous ML algorithms have been proposed to detect ASD. Most algorithms are suitable for static images such as CT scans and sMR images. Compared with static images, clinicians ASD abnormalities can more easily detect ASD abnormalities in 3D images and fMRI. Due to the above limitations, ASD identification becomes difficult and leads to a wrong diagnosis. A few researchers have proposed 3D-based DL algorithms. However, these algorithms are computationally intensive and require substantial memory resources. Also, these algorithms achieve lower accuracy than 2D-based algorithms. To overcome the aforementioned limitations, a machine learning ML) framework is proposed in this paper.

Numerous researchers have proposed numerous ML and DL techniques to address the various challenges in ASD detection. The novelty of the work is shown below.

- In this study, a novel 3D ResNet50 architecture is proposed to identify spatio-temporal features from fMRI images. Conventional 2D CNNs are suitable for static images, such as sMR images. But these 2D-based architectures fail to extract features from fMRI slices.
- In this work, the proposed 3D-ResNet50 is integrated with ML algorithms such as SVM, RF, LR, and KNN. In general, 3D-based architectures provide lower accuracy than 2D-based architectures. To improve accuracy, the proposed DL algorithm is integrated with ML algorithms. This is the first ML framework integrated with a 3D-DL architecture with ML algorithms.
- The proposed ML framework leverages the strengths of 3D-ResNet 50 and ML algorithms. 3D-ResNet 50 extracts complex functional patterns of the brain, and ML algorithms use these features to classify ASD controls.

This paper follows a specific organization, including a thorough review of previous ASD classification research and examinations of neuroimaging and machine learning strategies, as presented in Section II. The proposed framework details its operations in Section III by integrating 3D-ResNet50 as a deep feature extractor that works with ML algorithms for classification operations. Section IV covers the results and discussions, and Section V, accompanied by a conclusion and future scope.

2. Related work

Recent studies on Autism Spectrum Disorder (ASD) diagnostics and treatments have demonstrated significant advancements in the utilization of machine learning and technology. Hasan et al. [9] presented a machine learning-based framework using Support Vector Machines for early ASD detection, highlighting the necessity of a more diverse dataset to achieve better generalization. Wang et al. [10] evaluated the status of Electroencephalogram (EEG) and MRI technology used in ASD diagnosis, concluding that there was no standardization among the research studies. Liang et al. [11] combined CNN networks with prototype learning methods to classify brain functional networks using fMRI, but its practical application is restricted due to the high computational cost. Kohli et al. [12] reviewed the effects of intelligent technologies on the early detection of ASD, indicative of mobile technologies, but also described the troubles with integrating these innovative solutions in clinical use.

Yang et al. [13] proposed structural MRI biomarkers for ASD with multi-class activation mapping models to improve feature extraction and visualization, identifying critical brain regions affected by ASD. However, the study suggests the need for validation across broader demographic groups to ensure the biomarkers' universality and reliability. Ashraf et al. [14] applied deep learning through transfer learning approaches to analyze brain imaging data for early-age ASD detection, integrating IoT technologies for widespread application. This study underscores the potential of transfer learning to overcome the scarcity of large, annotated datasets in ASD research. However, it requires more comprehensive studies to confirm the findings across various populations. Karim et al. [15] presented an analytical study on the prediction of ASD meltdowns using ML techniques, which are acute emotional dysregulation incidents common among individuals with ASD. This research uses predictive models to suggest proactive strategies for controlling ASD symptoms while also emphasizing the difficulty of incorporating these models into daily practice due to diverse meltdown triggers and individual variations. Sadiq et al. [16] introduced a non-oscillatory connectivity approach to classify ASD subtypes using resting-state fMRI, utilizing advanced machine learning techniques like SVM. Their approach has shown a potential to differentiate between different complex ASD subgroups like Asperger’s disorder and pervasive developmental disorder, but stresses the necessity for larger sample sizes for validation.

Table 1. Summary of the reviewed deep learning studies

Study	Modality	Participants	Methods	Biomarkers	Best Accuray
Heinsfeld et al. (2018) [4]	fMRI	NASD = 530, ASD = 505	Deep Neural Network	A distributed network between anterior and posterior brain areas is negatively correlated.	70%
Jahani et al. (2024) [17]	sMRI & fMRI	NASD = 351, ASD = 351	3D-DenseNet	Abnormal connectivity was found in the cortical areas and thalamus.	72%
Thomas et al. (2020) [18]	fMRI	NASD = 542, ASD = 620	3D-CNN	An abnormal Regional Homogeneity was found in bilateral middle temporal gyri and The right parahippocampal gyrus of ASD controls.	66%
Dong et al. (2025) [19]	sMRI & fMRI	ASD = 467, NASD = 403	Edge-variational graph convolutional networks (EV-GCN)	Altered Functional Connectivity in the left and right Temporal Cortex of ASD controls.	72.2%
Ali et al. (2022) [20]	sMRI	NASD = 336, ASD = 328	Neural Network	Abnormal cortical folding pattern found in ASD controls.	71.6%
Zheng et al. (2025) [21]	fMRI	NASD = 111, ASD = 103	Dual Branch-Autoencoder	Functional connectivity is altered in the Left amygdala and right posterior cingulate gyrus.	70.7%
Almuqhim et al. (2021) [22]	fMRI	NASD= 530, ASD = 505	ASD -SAENet	Abnormal connectivity was found in the parahippocampal, left fusiform gyrus, and right hippocampus.	70.8%
Jung et al. (2023) [23]	fMRI	NASD = 462, ASD = 418	Stacked Autoencoder	Attenuated functional connectivity is identified in the right thalamus and lateral occipital cortex.	78.1%
Wang et al. 2019 [24]	fMRI	NASD = 255, ASD = 276	Stacked Sparse Auto Encoder	Attenuated functional connectivity is identified between the frontal pole and the temporal fusiform cortex	75.27%

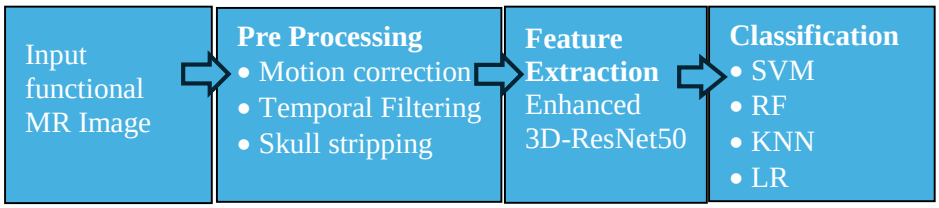

Fig. 1 Block diagram of proposed Machine Learning framework

Mohi-ud–Din et al. [24] detected ASD classification using EEG signals and 1D CNNs and proved the effectiveness of 1D CNNs in capturing temporal information and features in EEG time-domain signals for ASD diagnosis. Their analysis indicates that Deep Learning can significantly boost diagnostic performances, but the study indicates that model overfitting requires proper optimization methods and precision adjustment for success. Han et al. [25] have also used a multimodal approach by combining EEG, Eye-Tracking (ET), and neuroimaging data to diagnose ASD in children. The research applied stacked denoising autoencoders as a feature extraction and fusion method, which proved that combining multiple data types leads to better diagnostic outcomes.

Integrating complex multimodal data with advanced Machine Learning Frameworks creates challenges for successful clinical use. Liang et al. [26] developed an SVM classification system for identifying self-stimulatory behaviours in ASD patients by adopting explainable temporal coherency deep features. The system merges unsupervised deep learning techniques to discover temporal patterns in behavioural information, creating a new method for computationally analysing data behaviour. The results show promise, but individuals' unique behavioural patterns create difficulties when applying these frameworks to all cases.

Al-Hiyali et al. [27] combined the wavelet transform with transfer learning to classify BOLD fMRI signals to identify ASD. Their method improves feature extraction by converting the time series data to a scalable domain, using architectures like DenseNet201 and GoogleNet to increase the classification accuracy. This study demonstrates the benefit of hybrid methods in improving the interpretability of fMRI data, but consistent results over different populations remain a crucial step still to be accomplished. Rahman et al. [28] presented an in-depth review of the automated methods that use human activity analysis to diagnose ASD.

The review presents a variety of ML approaches for behavioural data analysis to diagnose ASD and also observes that combining multiple behavioural predictors can be more accurate. However, the review also highlights the need for standardized datasets and better validation approaches to take these technologies to the next level. Zhang et al. [29] investigated the assessment of symptom severity of ASD from EEG metrics.

Using EEG to examine the topology of the functional brain network, their study found network metrics that are associated with levels of ASD severity. This approach is also helpful in developing customized treatment plans and clarifying the neurobiological cause of ASD. The primary points raised are the lack of uniform standards in healthcare and the inconsistent quality of EEG signals.

The literature survey highlights the potential of ML and DL algorithms for ASD classification. However, the following gaps remain:

- Diagnosis methods like ADI-R and ADOS have long questionnaires and require certified trainers for proper assessment. Thus, a more accurate and faster method for diagnosing ASD is needed.
- Existing ML-based algorithms heavily depend on handcrafted features. Sometimes, handcrafted features can mislead the diagnosis of ASD for complex images like fMRI images. These algorithms are not always a viable solution.
- Most researchers use fMRI to identify functional abnormalities in patients with ASD. In 2D-DL algorithms, such as 2D-CNNs, some spatial information is lost. In the 2D-CNN algorithm, fMRI data are divided into 2D images, breaking the original volumetric relationships between regions. 3D architectures more effectively determine functional connectivity patterns than 2D architectures.

3. Proposed Method

The proposed framework uses Deep Learning and Machine Learning to improve ASD diagnosis by assessing Functional Magnetic Resonance Imaging (fMRI) data. The framework divides its approach into preprocessing, feature extraction, and classification. The preprocessing phase works on the ABIDE-I dataset, which contains resting-state fMRI scans from several international sites, by performing standardization to reduce differences between different imaging protocols [30]. Data preprocessing removes skull compartments and measures motion artefacts while normalizing spatial coordinates before smoothing features to create standardized, high-quality extracted data. Diminution procedures remove lazy data while maintaining crucial neurological patterns for classification.

The proposed 3D-ResNet50 architecture is a feature extractor that obtains spatial and temporal data features from preprocessed fMRI datasets. An innovative residual learning technique built into 3D-ResNet50 permits the successful extraction of hierarchical features while resolving gradient vanishing problems, so it operates on high-dimensional neuroimaging information [31]. The resultant feature maps show complex brain connectivity patterns because these patterns enable successful discrimination between ASD patients and control individuals.

The proposed algorithm uses ML classifiers to process the features extracted by 3D-ResNet50 to establish group affiliations between ASD and controls. ML algorithms prove suitable for the study because they can efficiently manage high-dimensional data distribution and establish optimal decision boundaries for high generalization performance, as shown in Figure 1. Cross-validation methods enable the

classifier to undergo training and validation sessions that validate the reliability of its model.

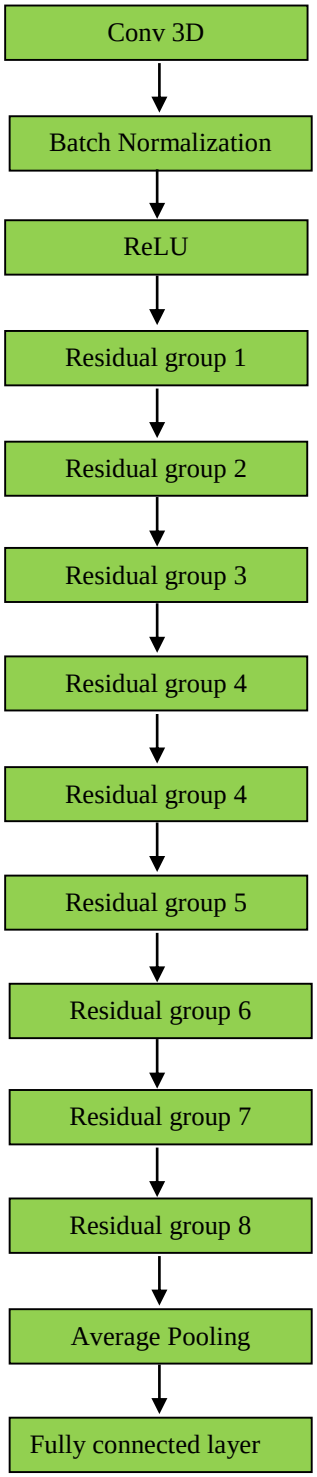

Fig. 2 Block diagram of 3D-ResNet50

The low-frequency fluctuations of resting-state brain activity are isolated by applying a band-pass filter that retains signals between 0.01 and 0.1 Hz. The Craddock 200 (CC200) atlas is employed to develop functional connectivity matrices through 200 Regions of Interest (ROIs). The proposed framework uses 3D-ResNet50 to diagnose ASD from controls based on fMRI data, as illustrated in Figure 2. The 3D-ResNet50 is an enhancement of ResNet50 for volumetric data, such as fMRI. The method enables deeper network learning through residual learning, thereby maintaining high performance standards. An enhanced 3D-Resnet50 architecture details are shown in Table 2.

3.1. Input and Initial Convolution

The architecture begins with an input 3D fMRI image volume, which is passed through a first 3D convolutional layer with a kernel size of 3x3x3. This layer retrieves spatial and temporal properties from the input volume, applying a convolution operation that is defined as in (1):

$$Y(i,j,k) = \sum_m \sum_n \sum_p X(i+m, j+n, k+p) \cdot W(m,n,p) + b \quad (1)$$

Where Y(i, j, k) is the output of the 3D CNN, X(i+m, j+n, k+p) is the input tensor, W(m,n,p) is the weight tensor, and b is the bias.

The fundamental structure of 3D-ResNet50 comprises four residual groups, each consisting of multiple convolutional blocks and identity blocks.

This 3D-ResNet50 architecture obtains spatial and temporal elements from fMRI data using multiple layers, including convolutional blocks, identity blocks, skip connections, pooling layers, and fully connected layers for ASD classification—convolutional block functions whenever feature maps get expanded or reduced in both sizes during times of down-sampling.

The 3D Convolutional Layer operates on three dimensions to analyze volumetric data. Then, the model utilizes Batch Normalization to normalize the convolutional outputs, allowing training to run more efficiently. The definition of the batch normalization operation is:

$$\hat{X} = \frac{X-\mu}{\sqrt{\sigma^2+\epsilon}} \cdot \gamma + \beta \quad (2)$$

Here μ and σ^2 are the mean and variance of the batch, ϵ is a small constant for numerical stability, γ and β are learnable parameters. The initial value of γ is 1, and β is 0. γ and β are used to improve the model performance and stability.

The identity block extracts more features that match input and output sizes while sustaining residual connections.

This identity block functions similarly to the convolutional block through 3D convolutions and contains

batch normalization and ReLU activation while connecting both the input and the last layer's output. The residual mapping method addresses the vanishing gradient issue, allowing deeper networks to efficiently learn for fMRI ASD diagnosis.

The network can bypass layers through skip connections and directly add input to transformed outputs because of this formula:

$$Output = F(X) + X \tag{3}$$

Here, X is the input and F(X) is the residual function. The convolutional layers transform the input data into the output pattern represented by $F(X)$.

$$F = W \cdot X + b \tag{4}$$

Where W is the weight matrix, b is the bias, and X is the input feature vector.

$$P(y = c) = \frac{exp(z_c)}{\sum_j exp(z_j)} \tag{5}$$

Where z_c is the output score for class c, z_j is the scores for all classes (j=1,2,…c) and $P(y = c)$ is the probability of the input belonging to class c.

3.2. Classification Using Machine Learning Algorithms

The 3D-ResNet50 architecture performs feature extraction, which enables various ML algorithms to classify extracted features. These algorithms include SVM, KNN, RF, and LR. Each algorithm employs its own method to distinguish between the extracted features of individuals with ASD and those of healthy controls.

3.2.1. Support Vector Machine

SVM is a method of supervised learning that finds the best hyperplane for a complete separation of two classes (ASD and Controls) in high-dimensional space. The optimal problem of SVM is expressed as in (6) and (7),

$$\min_{w,b} \frac{1}{2} \|w\|^2 + c \sum_{i=1}^{n} \xi_i \tag{6}$$

Subject to:

$$y_i(w \cdot x_i + b) \geq 1 - \xi_i, \xi_i \geq 0 \tag{7}$$

Where w is the weight vector, b is the bias term, c is the regulation parameter, ξ_i Are slack variables in case of the inflation of non-separable data, y_i Are the class marks (the class marks are: +1, for ASD; −1, for controls) and x_i is a feature vector.

The kernel employed in this study is the Radial Basis Function (RBF) kernel, as in (8):

$$K(x_i, x_j) = exp(-\gamma \| x_i - x_j \|^2) \tag{8}$$

Where γ stands as the kernel parameter, x_i and x_j These are input feature vectors. The SVM model demonstrates excellence in high-dimensional analysis and shows resistance to overfitting, which makes it suitable for ASD classification.

Table 2. Enhanced 3D-ResNet50 architectural parameters

Group	Layer	Architecture
Conv3D	Conv3D	3x3x3, 64, stride (1, 2, 2)
Residual Group 1	Conv 3D_1-1	1x1x1, 64
	Conv 3D_1-2	3x3x3, 64
	Conv 3D_1-3	1x1x1, 256
	Conv 3D_1-4	1x1x1, 256
Residual Group 2	Conv 3D_2-1	1x1x1, 64
	Conv 3D_2-2	3x3x3, 64
	Conv 3D_2-3	1x1x1, 256
Residual Group 3	Conv 3D_3-1	1x1x1, 128
	Conv 3D_3-2	3x3x3, 128, stride (2, 2, 2)
	Conv 3D_3-3	1x1x1, 512
	Conv 3D_3-4	1x1x1, 512, stride (2, 2, 2)
Residual Group 4	Conv 3D_4-1	1x1x1, 128
	Conv 3D_4-2	3x3x3, 128
	Conv 3D_4-3	1x1x1, 512
Residual Group 5	Conv 3D_5-1	1x1x1, 256
	Conv 3D_5-2	3x3x3, 256, stride (2, 2, 2)
	Conv 3D_5-3	1x1x1, 1024
	Conv 3D_5-4	1x1x1, 1024, stride (2, 2, 2)
Residual Group 6	Conv 3D_6-1	1x1x1, 256
	Conv 3D_6-2	3x3x3, 256
	Conv 3D_6-3	1x1x1, 1024
Residual Group 7	Conv 3D_7-1	1x1x1, 512
	Conv 3D_7-2	3x3x3, 512, stride (2, 2, 2)
	Conv 3D_7-3	1x1x1, 2048
	Conv 3D_7-4	1x1x1, 2048, stride (2, 2, 2)
Residual Group 8	Conv 3D_8-1	1x1x1, 512
	Conv 3D_8-2	3x3x3, 512
	Conv 3D_8-3	1x1x1, 2048

3.2.2. K-Nearest Neighbors (KNN)

KNN uses a non-parametric approach for classification, wherein points obtain their class label through the majority vote of their k-nearest neighbors. The determination of data point distance involves the application of the Euclidean distance calculation shown in (9):

$$d(x_i, x_j) = \sqrt{\sum_{m=1}^{n} (x_{i,m} - x_{j,m})^2} \tag{9}$$

Where $x_{i,m}$ and $x_{j,m}$ Are feature vectors, n is the number of features.

KNN is also simple and effective, but computationally complex for big data. It depends highly on the value of k and the distance metric.

3.2.3. Random Forest

A Random Forest is a tree-structured model in which each node is a decision based upon input features, each branch represents a decision result, and each leaf node represents the label class. The tree is built by iteratively dividing the data set into features that yield the highest information gain or Gini impurity. Random Forests are interpretable and can handle non-linear relationships, but they are prone to overfitting.

3.2.4. Logistic Regression

Logistic Regression functions as a linear system that performs binary classification. The model applies a logistic function to calculate class probability as defined in (10):

$$P(y = 1|x) = \frac{1}{1+\exp(-(w.x+b))} \quad (10)$$

Where w is the weight vector, b is the bias term, x is the feature vector. The model is trained by minimizing the log loss, which is defined as in (11):

$$L(w, b) = -\sum_{i=1}^{n} [y_i log(P(y_i = 1 \mid x_i)) \quad (11)$$

Where w is the weight vector, x_i is a feature vector, y_i is the class label, and b is the bias term. Logistic Regression is efficient and straightforward, but it models a linear relationship between results in features and the class's log odds.

4. Results and Discussion

The enhanced 3D-ResNet50 framework evaluated information from the 871 preprocessed resting-state fMRI scans distributed across 17 ABIDE-I international sites. Despite conventional CNN-based and 3D-CNN methods, the model demonstrated 90% accuracy for ASD classification. The model showed enhanced performance for the NYU site, with a 97% accuracy rating, because it could effectively adapt to reduced site-specific variations.

The combination of 3D-ResNet50 with SVM produced both effective spatial-temporal feature learning and created a sturdy decision border that eliminates the typical deep learning flaws connected to using neuroimaging data independently.

Different performance measures, including precision, recall, and F1-score, proved the reliability of this framework across datasets by showing enhanced generalization ability in multi-site data assessments. Deeper network training and better representation learning became possible because residual learning and skip connections resolved the vanishing gradient problem. Problems persist in the framework concerning its ability to handle imaging protocol differences and variations in scanner resolution and sample distribution patterns because these factors impact consistency in network performance.

Table 3. Performance of the proposed 3D-ResNet50 combined with different ML algorithms

Method	Accuracy (%)	Sensitivity (%)	Specificity (%)	F1-Score
3D-ResNet + SVM	90.00	80.91	76.12	69.96
3D-ResNet50 + RF	78.00	78.89	69.10	60.43
3D-ResNet50 + KNN	70.00	71.65	74.34	66.87
3D-ResNet50 + LR	85.00	69.71	67.65	70.43

The proposed enhanced 3D-ResNet50 model utilized SVM, RF, KNN, and LR as machine learning classifiers for assessment, as shown in Table 3. Records show that the 3D-ResNet50 + SVM system yielded an accuracy rate of 90%, proving its ability to classify ASD subjects from control groups precisely.

This 3D ResNet combination surpassed other models with a detection accuracy of 80.43%, which reflects its ability to accurately identify ASD cases together with 76.12% specificity and 69.96% F1-score, which indicates balanced performance. The accuracy of the Random Forest (RF) classifier reached 78%, yet its specificity dropped to 69.10%, causing more false results to occur. The KNN-based model achieved 70% accuracy while having lower sensitivity values of 71.65% and an F1-score of 66.87%, which suggests difficulties in understanding neuroimaging patterns in this model. The accuracy achieved by Logistic Regression (LR) reached only 85%, which was accompanied by poor sensitivity measurement (69.71%) and specificity (67.65%) to demonstrate ineffective performance in high-dimensional fMRI data analysis. SVM is the top choice in ASD classification when integrated with 3D-ResNet-50because it appropriately processes deep features and averts overfitting problems to establish reliability in ASD detection.

Different institutions within the ABIDE-I dataset demonstrated varying results in using 3D-ResNet-50 + SVM because of their distinct data collection protocols and magnetic resonance imaging parameters, as shown in Table 4.

Table 4. Site-Wise results for enhanced 3D-ResNet50 + SVM

Site	Accuracy (%)	Sensitivity (%)	Specificity (%)	F1-Score
CALTECH	86.40	86.40	81.20	78.89
CMU	88.90	80.32	71.10	86.10
KKI	78.90	81.54	86.44	87.32
LEUVEN	85.65	87.23	79.89	74.74
MAX MUN	88.43	78.65	82.22	68.19
NYU	97.00	93.10	96.55	89.01
OHSU	94.11	89.97	92.98	88.88
OLIN	94.54	91.11	76.34	70.94
PITT	91.11	87.88	71.11	68.91
SBL	90.09	92.32	90.09	73.01
SDSU	79.99	80.12	79.94	74.44
STANFORD	77.77	81.74	69.12	64.96
TRINITY	94.43	90.07	89.99	88.11
UCLA	87.86	81.45	76.75	70.04
UM	87.34	90.01	89.87	67.69
USM	83.33	80.43	91.04	76.18
YALE	95.98	93.45	86.41	81.71

Table 5. Site-wise results for enhanced 3D-ResNet50 + random forest

Site	Accuracy (%)	Sensitivity (%)	Specificity (%)	F1-Score
CALTECH	77.21	75.13	81.11	78.43
CMU	74.14	87.78	82.34	70.35
KKI	84.42	94.72	93.57	91.67
LEUVEN	93.99	90.65	82.56	88.35
MAX MUN	80.67	89.23	92.63	79.76
NYU	95.00	90.32	92.99	80.43
OHSU	90.01	83.67	93.08	79.99
OLIN	89.99	92.22	87.54	82.94
PITT	90.07	94.76	80.01	77.77
SBL	92.24	84.49	90.38	90.07
SDSU	74.56	81.74	75.75	79.72
STANFORD	89.93	85.25	79.34	75.01
TRINITY	89.99	94.45	78.78	73.49
UCLA	90.94	91.78	86.84	79.34
UM	92.22	80.91	80.02	79.34
USM	94.08	79.56	92.46	75.76
YALE	90.10	95.14	76.32	85.86

Testing on the NYU site delivered 97% overall accuracy, with a sensitivity of 93.10% and specificity of 96.55%, demonstrating an excellent classification performance balance. Data collected from OHSU, OLIN, TRINITY, and YALE produced high classification performance rates at 94.11 per cent, 94.54 per cent, 94.43 per cent, and 95.98 per cent, respectively. CMU achieved 88.90% accuracy, followed by MAX MUN at 88.43%, then UCLA at 87.86%, and UM at 87.34%. At the same time, CALTECH reached 86.40% accuracy, and LEUVEN obtained 85.65%. STANFORD (77.77%) and SDSU (79.99%) showed reduced accuracy results because imaging protocols exhibited higher levels of variation. Different sites recorded F1-scores that spanned between 64.96% (STANFORD) to 89.01% (NYU), showing that dataset quality and homogeneity directly influenced classification effectiveness.

Different ABIDE-I sites demonstrated distinct classification abilities through the 3D-ResNet50 + Random Forest (RF) framework, resulting in NYU (95%) leading among NYU, LEUVEN (93.99%) performing second, YALE (90.10%), and PITT (90.07%) following closely. In comparison, KKI (84.42%) and MAX MUN (80.67%) displayed good results, with KKI achieving maximum

sensitivity (94.72%), as shown in Table 5. The remaining sites, like SDSU (74.56%) and CMU (74.14%), exhibited reduced performance, likely due to site-specific factors. The KKI site obtained the highest sensitivity rating (94.72%), achieving 84.42% accuracy.

The sites SDSU and CMU showed performance at 74.56% and 74.14%, respectively, because their data showed high variability, while their imaging protocols differed from those of other sites. The F1-score measurements from CMU were lowest at 70.35%, while KKI produced the highest F1-score at 91.67%. The scores also included LEUVEN at 88.35% and OLIN at 82.94%. Random Forest classifiers demonstrated comparable accuracy but exhibited site-dependent performance discrepancies because their specificity ranged between 75.75% and 93.57%, producing more incorrect optimistic predictions than SVM classifiers.

The 3D-ResNet50 + KNN approach produced excellent results at multiple sites by achieving the highest accuracy rates of 92% for UM, 91% for TRINITY, 86.96% for CALTECH, and 86.32% for YALE because KNN effectively detected site-specific neuroimaging patterns, as shown in Table 6. Another set of clinical data from LEUVEN obtained 93.33% accuracy, and KKI obtained 92.47% accuracy, which showed a balanced performance between sensitivity and specificity measures. The features showed reduced consistency at NYU and OLIN due to imaging variability, causing their accuracy rates to drop to 76.19% and 76.97%, respectively.

The F1-scores displayed significant variability, with STANFORD reaching 71.05% while SBL scored the highest at 91.01% among sites. KNN achieved overall good performance yet demonstrated inconsistent results between sites, indicating its susceptibility when applied to distributions of neuroimaging data in high dimensions, which affects its general applicability compared to SVM-based classification methods. The 3D-ResNet50 + Logistic Regression (LR) framework generally obtained poor performance results due to its challenges working with high-dimensional fMRI data. In general, LR methods are suitable for 2D images.

Table 6. Site-wise results for enhanced 3D-ResNet50 + KNN

Site	Accuracy (%)	Sensitivity (%)	Specificity (%)	F1-Score
CALTECH	86.87	86.51	92.81	89.37
CMU	84.17	95.45	92.33	76.66
KKI	92.47	84.42	83.55	89.68
LEUVEN	93.33	94.44	91.85	88.85
MAX MUN	90.69	92.22	82.69	89.06
NYU	92.00	79.25	81.98	89.93
OHSU	86.06	93.69	83.01	89.97
OLIN	76.97	72.82	97.55	72.95
PITT	83.59	84.97	90.91	79.78
SBL	90.02	80.41	96.38	91.01
SDSU	79.58	91.79	95.85	89.79
STANFORD	89.91	84.28	75.37	71.05
TRINITY	89.96	91.44	88.98	84.29
UCLA	91.93	81.79	95.83	89.31
UM	91.00	91.49	94.24	77.23
USM	91.91	71.59	82.43	86.51
YALE	86.32	85.14	96.32	75.38

Among the sites, NYU achieved the best overall accuracy at 90%, and CALTECH achieved 89.85% accuracy. Yet, CMU maintained adequate specificity at 78.23%, while CALTECH showed excellent sensitivity at 96.13% to effectively detect ASD cases, as shown in Table 7. The sites of NYU and OLIN demonstrated moderate success. Still, their accuracy levels were at 89.71% and 84.51%, respectively, while the sites STANFORD USM and YALE showed the lowest detection rates with results at 67.79%, 63.39% and 65.95%, respectively. The F1 scores between sites showed substantial differences because OHSU achieved 58.48% while NYU obtained 82.12% accuracy. The sensitivity rates showed irregular patterns because OHSU (69.92%) and SDSU (60.19%) misidentified ASD subjects, which resulted in possible inaccuracies.

The learning progress of the model appears through the Training vs Validation Accuracy Curve, which presents the blue solid line for training accuracy and the red dashed line for validation accuracy for 25 epochs, as shown in Figure 3.

Table 7. Site-wise results for enhanced 3D-ResNet50 + logistic regression

Site	Accuracy (%)	Sensitivity (%)	Specificity (%)	F1-Score
CALTECH	89.85	96.13	91.13	70.19
CMU	84.21	72.71	78.23	70.10
KKI	70.09	75.51	77.93	80.03
LEUVEN	80.51	77.29	69.81	65.73
MAX MUN	70.43	68.64	62.29	65.91
NYU	90.00	87.40	77.76	82.12
OHSU	77.61	69.92	62.98	58.48
OLIN	84.51	81.18	66.39	60.91
PITT	71.15	67.89	81.41	68.94
SBL	72.09	70.33	68.02	70.09
SDSU	69.95	60.19	69.94	64.47
STANFORD	67.79	61.78	60.19	61.94
TRINITY	64.49	70.09	80.11	80.17
UCLA	77.89	71.47	74.74	71.02
UM	67.36	60.91	69.89	64.62
USM	63.39	67.95	61.94	66.19
YALE	65.95	63.85	66.44	61.09

The metrics begin with a progressive ascent as the model acquires essential patterns from the data. At epoch 20-25, the accuracy becomes stable, while training accuracy achieves approximately 88%, and validation accuracy levels are at 86%. Minor overfitting is normal for deep learning models, so a small gap exists between training and validation accuracy, while the overall performance shows adequate learning.

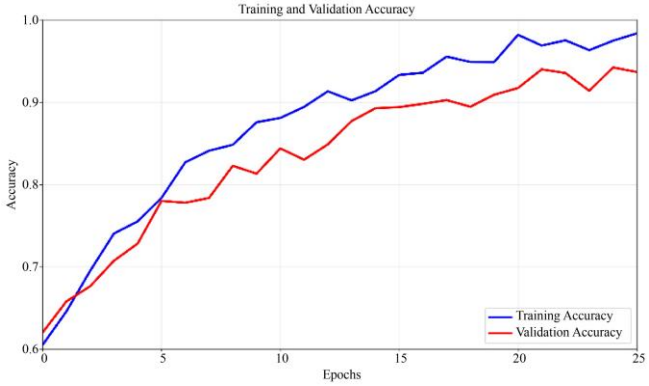

Fig. 3 Training and validation accuracy curve for enhanced 3D ResNet + SVM method using entire ABIDE-I preprocessed data

The dynamic variations in model performance provide a realistic assessment of generalization abilities for the 3D-ResNet50 + SVM proposed framework through this visualization tool. Figure 4 shows the model's training. The blue solid line represents training loss, while the red dashed line represents validation loss, which decreased steadily until both lines stabilized. The losses show initial high readings until they decrease steadily because the model effectively learns and reduces errors. After twenty-five epochs, the loss reaches equilibrium, which signifies that the model has achieved its ideal learning threshold. The model's training outcome achieves 0.1 loss, and validation reaches 0.15 loss, indicating a suitable fit and low overfitting potential.

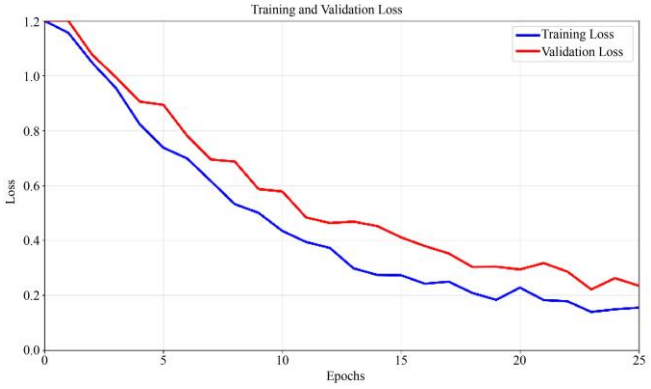

Fig. 4 Training and validation loss curve for enhanced 3D-ResNet50 + SVM method using entire ABIDE-I preprocessed data

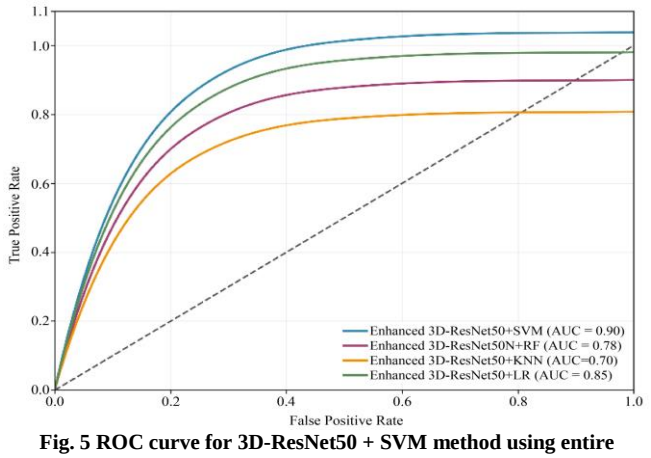

Fig. 5 ROC curve for 3D-ResNet50 + SVM method using entire ABIDE-I preprocessed data

The ROC Curve of Figure 5 demonstrates how different models (LR, SVM, RF, KNN) perform their classification tasks by analyzing the complete ABIDE-I dataset (871 subjects). SVM delivered the best AUC of 0.85 because of its excellent discrimination capabilities between subjects with ASD and controls.

The classification results showed that logistic regression reached AUC 0.79, random forest reached AUC 0.75, and KNN obtained a lower AUC of 0.70. Models with zero discrimination ability have an AUC value of 0.50, equal to the random guess baseline. SVM emerges as the most effective classification model for fMRI data-based ASD classification because its reported AUC values are the highest.

The Training vs. Validation Accuracy Curve for the NYU site extends for 40 epochs, as shown in Figure 6. The learning process demonstrates solid performance because training accuracy (blue solid line) and validation accuracy (red dashed line) improve consistently to reach 97% and 95%, respectively. The escalating performance indicates minimal dimension overfitting occurred because the validation accuracy traces very closely after the training curve.

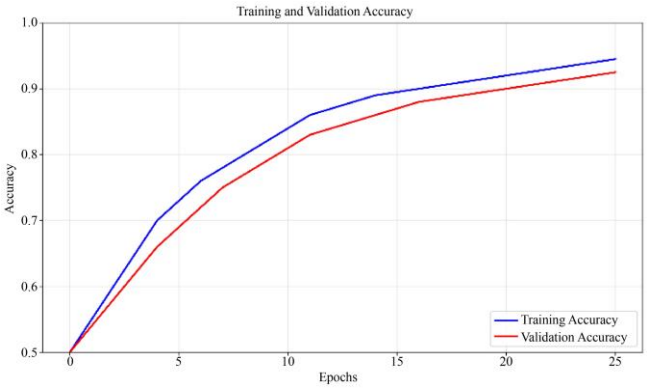

Fig. 6 Training and validation accuracy curve for enhanced 3D-ResNet50 + SVM method using the NYU site

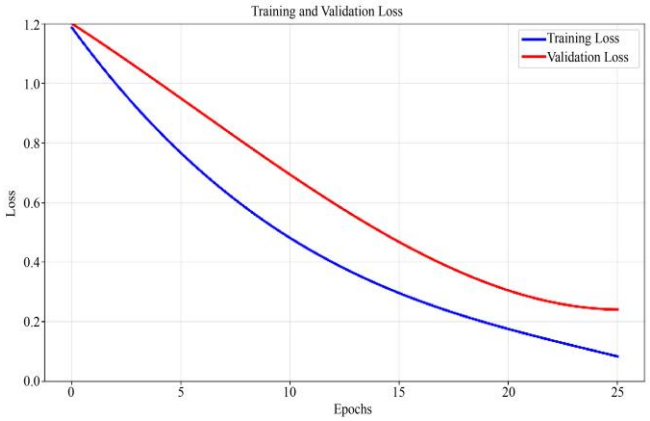

Fig. 7 Training and validation loss curve for enhanced 3D ResNet + SVM method using the NYU site

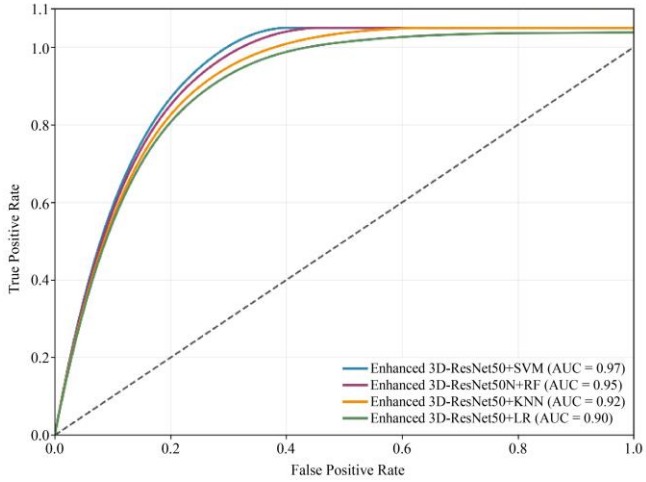

Fig. 8 ROC curve for 3D-ResNet50 + SVM method using the NYU site

The Training vs Validation Loss Curve of the NYU site in Figure 7 shows a continuous loss reduction for 40 epochs, which indicates successful learning. The training loss (Blue Solid Line) shows consistent descent, whereas validation loss (Red Dashed Line) stabilizes near 0.08 while training loss approaches 0.0. Due to its smooth loss reduction pattern, the model achieves strong convergence, low overfitting, and optimal performance at the NYU site.

Table 8. Performance comparison of the proposed machine learning framework with previous studies on the ABIDE-1 database

Study	Accuracy (%)	Participants	Method
Sherkatghanad et al. [32]	70.22	1112	CNN
Thomas et al. [18]	66	1162	3D-CNN
Wang et al. [33]	71.60	1057	Graph convolutional network (GCN)
Deng et al. [34]	74.53	1112	Ensemble 3D-CNN
Sabegh et al. [35]	73.53	1112	CNN
Liu et al. [36]	75.20	1112	Multi-atlas deep ensemble (MADE) network
Proposed method (for entire ABIDE-I data)	90	1112	3D-ResNet50 + SVM
Proposed method (for NYU site)	97	184	3D-ResNet50 + SVM

Figure 8 displays the ROC Curve assessment of different classification models, which include Logistic Regression (LR), Support Vector Machine (SVM), Random Forest (RF), and K-Nearest Neighbors (KNN) applied to the NYU site. Support Vector Machine revealed the best testing performance by generating an area under the curve of 0.95, demonstrating its strong capability to separate ASD from healthy controls. Random Forest achieved an AUC value of 0.85, and KNN reached an AUC of 0.85, and both provided good classification results. The models included Logistic Regression with an AUC of 0.80 and Random Forest with an AUC of 0.75, which exhibited moderate classification ability. A model lacking discrimination ability would perform at a random guess rate, which equates to an AUC of 0.5.

The accuracy assessment of the proposed 3D-ResNet50 + ML framework for ASD classification becomes more effective than earlier studies on ABIDE, as reported in Table 8. Existing CNN, 3D-CNN, and Graph Convolutional Networks (GCN) models achieved ASD classification accuracies between 66%, as reported by Thomas et al. (2020), and 75.20%, as observed by Liu et al. (2024). The ensemble of 3D-CNN achieved an accuracy of 74.53%, according to Deng et al. (2022).

However, Sabegh et al. (2023) and Wang et al. (2021) reported accuracies of 73.53% and 71.60%, respectively, using CNN and GCN. The proposed method produced superior results compared to existing works by reaching 87.14% accuracy on the entire ABIDE-I dataset and an outstanding 97.40% accuracy on the NYU site through integrating 3D-ResNet50 for feature extraction and machine learning classifiers.The proposed machine learning ML) framework outperformed existing techniques. The summary of the existing algorithms is shown in Table 7. Thomas et al. proposed a 3D-CNN algorithm and achieved a 66% accuracy. In contrast, Sherkatghana et al proposed a 2D-CNN and achieved 70.22%. Compared to 3D-based CNN algorithms, the 2D-based CNN algorithm achieved good accuracy. Due to fewer parameters and reduced overfitting, the 2D-CNN achieved good results. The proposed ML framework achieved high accuracy by integrating 3D-ResNet50 with ML classifiers. The proposed 3D-ResNet50 efficiently extracts spatio-temporal features from fMRI images. These features are provided to the ML classifiers for classifying ASD controls. Remarkable results were achieved due to this DL and ML integration method.

5. Conclusion

The Neurodevelopmental condition, autism spectrum disorder, causes significant interference with how people communicate and interact socially and impacts their cognitive processing abilities. Behavioural assessments, which traditionally diagnose autism, use highly subjective and time-consuming methods that produce inconsistent results, thus requiring automated data-based solutions. The research designs an innovative ASD diagnostic structure using 3D-ResNet50 for extracting features while machine learning classifiers perform the classification operation on fMRI data collected from the ABIDE-I dataset. The proposed approach successfully reduces problems in high-dimensional fMRI data and site-specific variations in different imaging facilities. The feature extraction capabilities of the 3D-ResNet50-based approach surpassed those of conventional CNN and 3D-CNN since it avoided their generalization and overfitting weaknesses, thus enhancing ASD classification outputs. The evaluation of ABIDE-I data yielded 90% overall classification accuracy and 97% accuracy at the NYU site while surpassing all previous state-of-the-art methods.

The SVM classifier exploited deep features successfully during analysis and demonstrated the best AUC value (0.95) in ASD categorization. Research efforts for the upcoming years will concentrate on developing domain adaptation and transfer learning methods to boost the generalization of the proposed 3D-ResNet50 + ML system. Using multiple neuroimaging data methods (sMRI together with Diffusion tensor imaging and EEG) enables researchers to obtain additional information about brain connectivity structures, leading to better classification results. Implementing Explainable AI (XAI) methods will make models more interpretable, which will help clinicians use neurobiological indicators for specific clinical decisions. Physicians can execute automated ASD screening through cloud-based and edge-computing systems for real-time clinical deployment, which enables early diagnosis. The extraction of features and scalability improvement requires more validation on large independent datasets, graph-based approaches, transformer modelling, and self-supervised learning.

References

[1] I. Kamp-Becker et al., "Diagnostic Accuracy of the ADOS and ADOS-2 in Clinical Practice," *European Child & Adolescent Psychiatry*, vol. 27, pp. 1193-1207, 2018. [CrossRef] [Google Scholar] [Publisher Link]

[2] Jared A. Nielsen et al., "Multisite Functional Connectivity MRI Classification of Autism: ABIDE Results," *Frontiers in Human Neuroscience*, vol. 7, pp. 1-12, 2013. [CrossRef] [Google Scholar] [Publisher Link]

[3] Lizhen Shao et al., "Classification of ASD Based on fMRI Data with Deep Learning," *Cognitive Neurodynamics*, vol. 15, pp. 961-974, 2021. [CrossRef] [Google Scholar] [Publisher Link]

[4] Anibal Sólon Heinsfeld et al., "Identification of Autism Spectrum Disorder using Deep Learning and the ABIDE Dataset," *Neuroimage: Clinical*, vol. 17, pp. 16-23, 2018. [CrossRef] [Google Scholar] [Publisher Link]

[5] Meijie Liu, Baojuan Li, and Dewen Hu, "Autism Spectrum Disorder Studies Using fMRI Data and Machine Learning: A Review," *Frontiers in Neuroscience*, vol. 15, pp. 1-17, 2021. [CrossRef] [Google Scholar] [Publisher Link]

[6] Nurul Amirah Mashudi, Norulhusna Ahmad, and Norliza Mohd Noor, "Classification of Adult Autistic Spectrum Disorder using Machine Learning Approach," *IAES International Journal of Artificial Intelligence*, vol. 10, no. 3, pp. 743-751, 2021. [CrossRef] [Google Scholar] [Publisher Link]

[7] R. Abhinav Chaitanya et al., "Autism Spectrum Disorder Detection using Attention-Based CNN and ML Classifiers," *Procedia Computer Science*, vol. 258, pp. 4216-4227, 2025. [CrossRef] [Google Scholar] [Publisher Link]

[8] Alexandre Abraham et al, "Deriving Reproducible Biomarkers from Multi-site Resting-state Data: An Autism-based Example," *NeuroImage*, vol. 147, pp. 736-745, 2017. [CrossRef] [Google Scholar] [Publisher Link]

[9] S.M. Mahedy Hasan et al., "A Machine Learning Framework for Early-Stage Detection of Autism Spectrum Disorders," *IEEE Access*, vol. 11, pp. 15038-15057, 2023. [CrossRef] [Google Scholar] [Publisher Link]

[10] Zhiyong Wang et al., "Diagnosis and Intervention for Children with Autism Spectrum Disorder: A Survey," *IEEE Transactions on Cognitive and Developmental Systems*, vo. 14, no. 3, pp. 819-832, 2022. [CrossRef] [Google Scholar] [Publisher Link]

[11] Yin Liang, Baolin Liu, and Hesheng Zhang, "A Convolutional Neural Network Combined with Prototype Learning Framework for Brain Functional Network Classification of Autism Spectrum Disorder," *IEEE Transactions on Neural Systems and Rehabilitation Engineering*, vol. 29, pp. 2193-2202, 2021. [CrossRef] [Google Scholar] [Publisher Link]

[12] Manu Kohli, Arpan Kumar Kar, and Shuchi Sinha, "The Role of Intelligent Technologies in Early Detection of Autism Spectrum Disorder (ASD): A Scoping Review," *IEEE Access*, vol. 10, pp. 104887-104913, 2022. [CrossRef] [Google Scholar] [Publisher Link]

[13] Rui Yang et al., "Exploring sMRI Biomarkers for Diagnosis of Autism Spectrum Disorders Based on Multi Class Activation Mapping Models," *IEEE Access*, vol. 9, pp. 124122-124131, 2021. [CrossRef] [Google Scholar] [Publisher Link]

[14] Adnan Ashraf et al., "Analysis of Brain Imaging Data for the Detection of Early Age Autism Spectrum Disorder Using Transfer Learning Approaches for Internet of Things," *IEEE Transactions on Consumer Electronics*, vol. 70, no. 1, pp. 4478-4489, 2024. [CrossRef] [Google Scholar] [Publisher Link]

[15] Sara Karim et al., "A Review on Predicting Autism Spectrum Disorder(ASD) meltdown using Machine Learning Algorithms," *2021 5th International Conference on Electrical Engineering and Information Communication Technology (ICEEICT)*, Dhaka, Bangladesh, pp. 1-6, 2021. [CrossRef] [Google Scholar] [Publisher Link]

[16] Alishba Sadiq et al., "Non-Oscillatory Connectivity Approach for Classification of Autism Spectrum Disorder Subtypes Using Resting-State fMRI," *IEEE Access*, vol. 10, pp. 14049-14061, 2022. [CrossRef] [Google Scholar] [Publisher Link]

[17] Ali Jahani et al., "Twinned Neuroimaging Analysis Contributes to Improving the Classification of Young People with Autism Spectrum Disorder," *Scientific Reports*, vol. 14, pp. 1-10, 2024. [CrossRef] [Google Scholar] [Publisher Link]

[18] Rajat Mani Thomas et al., "Classifying Autism Spectrum Disorder Using the Temporal Statistics of Resting-State Functional MRI Data With 3D Convolutional Neural Networks," *Frontiers in Psychiatry*, vol. 11, pp. 1-12, 2020. [CrossRef] [Google Scholar] [Publisher Link]

[19] Yilan Dong, Dafnis Batalle, and Maria Deprez, "A Framework for Comparison and Interpretation of Machine Learning Classifiers to Predict Autism on the ABIDE Dataset," *Human Brain Mapping*, vol. 46, no. 5, pp. 1-20, 2025. [CrossRef] [Google Scholar] [Publisher Link]

[20] Mohamed T. Ali et al., "The Role of Structure MRI in Diagnosing Autism," *Diagnostics*, vol. 12, no. 1, pp. 1-28, 2022. [CrossRef] [Google Scholar] [Publisher Link]

[21] Qiang Zheng et al., "ConnectomeAE: Multimodal Brain Connectome-based Dual-branch Autoencoder and its Application in the Diagnosis of Brain Diseases," *Computer Methods and Programs in Biomedicine*, vol. 267, 2025. [CrossRef] [Google Scholar] [Publisher Link]

[22] Fahad Almuqhim, and Fahad Saeed, "ASD-SAENet: A Sparse Autoencoder, and Deep-Neural Network Model for Detecting Autism Spectrum Disorder (ASD) Using fMRI Data," *Frontiers in Computational Neuroscience*, vol. 15, pp. 1-10, 2021. [CrossRef] [Google Scholar] [Publisher Link]

[23] Wonsik Jung et al., "EAG-RS: A Novel Explainability-Guided ROI-Selection Framework for ASD Diagnosis via Inter-Regional Relation Learning," *IEEE Transactions on Medical Imaging*, vol. 43, no. 4, pp. 1400-1411, 2023. [CrossRef] [Google Scholar] [Publisher Link]

[24] Canhua Wang, Zhiyong Xiao, and Jianhua Wu, "Functional Connectivity-based Classification of Aautism and Control using SVM-RFECV on rs-fMRI Data," *Physica Medica*, vol. 65, pp. 99-105, 2019. [CrossRef] [Google Scholar] [Publisher Link]

[25] Junxia Han et al., "A Multimodal Approach for Identifying Autism Spectrum Disorders in Children," *IEEE Transactions on Neural Systems and Rehabilitation Engineering*, vol. 30, pp. 2003-2021, 2022. [CrossRef] [Google Scholar] [Publisher Link]

[26] Shuaibing Liang et al., "Autism Spectrum Self-Stimulatory Behaviors Classification Using Explainable Temporal Coherency Deep Features and SVM Classifier," *IEEE Access*, vol. 9, pp. 34264-34275, 2021. [CrossRef] [Google Scholar] [Publisher Link]

[27] Mohammed I. Al-Hiyali et al., "Classification of BOLD FMRI Signals Using Wavelet Transform and Transfer Learning for Detection of Autism Spectrum Disorder," *2020 IEEE-EMBS Conference on Biomedical Engineering and Sciences (IECBES)*, Langkawi Island, Malaysia, pp. 94-98, 2021. [CrossRef] [Google Scholar] [Publisher Link]

[28] Sejuti Rahman et al., "Automated Detection Approaches to Autism Spectrum Disorder Based on Human Activity Analysis: A Review," *Cognitive Computation*, vol. 14, pp. 1773-1800, 2022. [CrossRef] [Google Scholar] [Publisher Link]

[29] Yangsong Zhang et al., "Predicting the Symptom Severity in Autism Spectrum Disorder Based on EEG Metrics," *IEEE Transactions on Neural Systems and Rehabilitation Engineering*, vol. 30, pp. 1898-1907, 2022. [CrossRef] [Google Scholar] [Publisher Link]

[30] A Di Martino et al., "The Autism Brain Imaging Data Exchange: Towards a Large-Scale Evaluation of the Intrinsic Brain Architecture in Autism," *Molecular Psychiatry*, vol. 19, no. 6, pp. 659-667, 2014. [CrossRef] [Google Scholar] [Publisher Link]

[31] Michelle Tang et al., "Deep Multimodal Learning for the Diagnosis of Autism Spectrum Disorder," *Journal of Imaging*, vol. 6, no. 6, pp. 1-11, 2020. [CrossRef] [Google Scholar] [Publisher Link]

[32] Zeinab Sherkatghanad et al., "Automated Detection of Autism Spectrum Disorder Using a Convolutional Neural Network," *Frontiers in Neuroscience*, vol. 13, pp. 1-13, 2020. [CrossRef] [Google Scholar] [Publisher Link]

[33] Lebo Wang, Kaiming Li, and Xiaoping P. Hu, "Graph Convolutional Network for fMRI Analysis based on Connectivity Neighborhood," *Network Neuroscience*, vol. 5, no. 1, pp. 83-95, 2021. [CrossRef] [Google Scholar] [Publisher Link]

[34] Jingsheng Deng et al., "Diagnosing Autism Spectrum Disorder Using Ensemble 3D-CNN: A Preliminary Study," *2022 IEEE International Conference on Image Processing (ICIP)*, Bordeaux, France, pp. 3480-3484, 2022. [CrossRef] [Google Scholar] [Publisher Link]

[35] Amin Majidzadeh Sabegh et al., "Automatic Detection of Autism Spectrum Disorder based on fMRI Images using a Novel Convolutional Neural Network," *Research on Biomedical Engineering*, vol. 39, pp. 407-413, 2023. [CrossRef] [Google Scholar] [Publisher Link]

[36] Xuehan Liu et al., "MADE-for-ASD: A Multi-Atlas Deep Ensemble Network for Diagnosing Autism Spectrum Disorder," *Computers in Biology and Medicine*, vol. 182, pp. 1-10, 2024. [CrossRef] [Google Scholar] [Publisher Link]